Robotica (2011) volume 29, pp. 421–432. © Cambridge University Press 2010
doi:10.1017/S0263574710000251

Validating extended neglect tolerance model for human robot interactions in humanoid soccer robots

R. E. Mohan†‡,*, W. S. Wijesoma‡, C. A. A. Calderon† and C. J. Zhou†

† *Advanced Robotics and Intelligent Control Centre, Singapore Polytechnic, 500 Dover Road, Singapore*
‡ *Division of Control & Instrumentation, School of Electrical and Electronics Engineering, Nanyang Technological University, Singapore. E-mail: eswwijesoma@ntu.edu.sg*

(Received in Final Form: June 1, 2010. First published online: July 7, 2010)

SUMMARY
Estimating robot performance in human robot teams is a vital problem in human robot interaction community. In a previous work, we presented extended neglect tolerance model for estimation of robot performance, where the human operator switches control between robots sequentially based on acceptable performance levels, taking into account any false alarms in human robot interactions. Task complexity is a key parameter that directly impacts the robot performance as well as the false alarms occurrences. In this paper, we validate the extended neglect tolerance model for two robot tasks of varying complexity levels. We also present the impact of task complexity on robot performance estimations and false alarms demands. Experiments were performed with real and virtual humanoid soccer robots across tele-operated and semi-autonomous modes of autonomy. Measured false alarm demand and robot performances were largely consistent with the extended neglect tolerance model predictions for both real and virtual robot experiments. Experiments also showed that the task complexity is directly proportional to false alarm demands and inversely proportional to robot performance.

KEYWORDS: Human robot teams; Robot performance; Task complexity; False alarm demand; Humanoid soccer robots; Autonomy modes.

1. Introduction

Growing popularity and increasing viable application domains has contributed to greater presence of robots in the commercial marketplace. Many of these applications require humans and robots to interact closely and work together towards a common goal. Some real life examples of such scenarios include edutainment, service, rescue and surgical robots)[1,2,3,23]. Robot autonomy is an essential component in these applications as it exempts human operators from the time-intensive control and decision-making processes. Most robotic applications for the commercial market can be categorized into tele-operation and semi-autonomous modes of autonomy. In tele-operation mode, the human operator guides the robot continuously until the given goal is accomplished. This mode requires complete attention of the human operator during the whole operation and every single decision is made by the operator and the robot has zero intelligence.[4,5] In semi-autonomous mode, the human and the robot collaboratively control parts of the functions required to accomplish the goal. The amount of functions left to the robot depends on the level of robot intelligence, in most scenarios the repetitive, low-level tasks are handled by robots and only few high-level tasks and decisions making steps are handled by humans.[6,7] Therefore, the operator work load is greatly reduced in semi-autonomous mode as compared to the tele-operation mode. The experiments presented in this paper were performed across the tele-operation and semi-autonomous modes of autonomy.

Robot performance in human robot teams is complex and multi-faceted reflecting the capabilities of the robot(s), the operator(s) and the quality of interactions.[8] The neglect tolerance model presented in ref. [9] is used as a general index for estimating robot performance in relation to autonomy in human robot interaction community. This model is employed in ref. [10] to predict the optimised number of robots that should be utilized in human robot teams and robot system effectiveness. Neglect tolerance model is applied in ref. [11] to estimate instantaneous robot performance, evaluate and compare three human robot interaction systems. The neglect tolerance model is applied in ref. [12] to evaluate human robot interaction systems with special focus on the role of a collaborative workspace in enabling mixed initiative interaction between humans and heterogeneous teams of robotic vehicles. Neglect tolerance model is also adopted in ref. [13] to derive model that approximates absolute autonomy and power in agent systems.

Neglect tolerance model is extended in ref. [14] to investigate human interaction in cooperating human robot teams within a realistically complex environment. Neglect tolerance model assumes ideal conditions while estimating performances, ignoring any false alarms due to erroneous interactions between the human operator and robot. But, in most real life applications erroneous interactions between the human operator and the robot are common due to uncertainties in both human operators as well as in robots. These erroneous interactions lead to false alarms which can be classified into two categories namely, the false

* Corresponding author. E-mail: MohanRajesh@sp.edu.sg

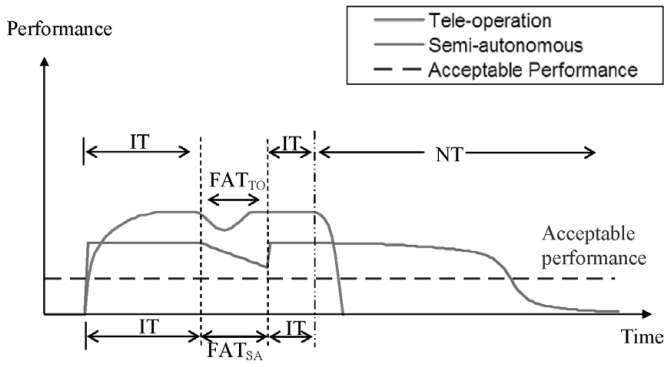
https://doi.org/10.1017/S0263574710000251 Published online by Cambridge University Press

positives wherein a robot rejects a 'correct' interaction and false negatives wherein a robot fails to reject an 'incorrect' interaction. False alarms negatively impact the performance of human robot teams. This zero false alarm assumption results in a less accurate estimation of robot attention demand and robot performance, not only leading to the operator's failure in accomplishing the task as scheduled due to higher attention demands in actual situation, but also leading to operator's inability to achieve the performance level set for that task due to the drop in performance attributed to the false alarms. In our earlier work,[15] we presented the extended neglect tolerance model to estimate robot performance taking into account the additional demands required due to false alarms. We also showed that the extended neglect tolerance model offers better estimations of robot attention demand, and robot performances as compared to neglect tolerance model.

The extended neglect tolerance model together with the metrics put forwards in this paper including, false positive interaction, false negative interaction, false alarm demand and extended robot attention demand can be used as a general metric for evaluating human robot interactions. Extended neglect tolerance model is applied in ref. [17] to estimate performance in search and rescue robotic operation and is also applied in ref. [16] to estimate the fan out in service robotic application. For any robotics applications, task complexity is one of the critical factors directly impacting the performance of the robot and occurrence of false alarms in human robot teams. In our previous work, we only experimented and estimated robot performance using the extended neglect tolerance model over a single task with no complexity variations. But, extended neglect tolerance model can be applied to any robotics application irrespective of the task complexity, robot platform, or domain. Neglect tolerance and interface efficiency are proportional to the task complexity, therefore deriving the influence of latter on robot performance and false alarm demands is necessary for the robot operators to better gauge and optimise resources for the robot task on hand. In this paper, we validate the extended neglect tolerance model for two real and virtual humanoid soccer robotic tasks with varying complexity levels across two levels of robot autonomy. We also present the impact of task complexity on robot performance estimations and false alarms demands. In this paper, we will first discuss the extended neglect tolerance model. In Section 3, we will present a brief description of our real and virtual Robo-Erectus Junior humanoid robots used in the experiments. In Section 4, we will present the experiments involving twenty test subjects to validate the extended neglect tolerance model for two tasks with varying level of complexities across two autonomy modes. Finally, Section 5 presents some concluding ideas.

2. The Extended Neglect Tolerance Model

The neglect tolerance model exploits neglect tolerance and interface efficiency parameters for estimating robot performance in human robot teams.[18,19,20] Neglect tolerance is a measure of how the robot's performance drops over time when the robot is neglected by the user. Interface efficiency



IT : Interaction Time
NT : Neglect Time
FAT_{TO} : False Alarm Time (Tele-operation)
FAT_{SA} : False Alarm Time (Semi-autonomous)

Fig. 1. Extended neglect tolerance model for measuring robot performance in human robot teams.

is a measure of how the robot's performance varies over time when the robot is being serviced by the human operator. The neglect tolerance model assumes zero erroneous interactions during robot operation while estimating robot performance in human robot teams. But, in most real life situations uncertainties in both human operator and the robots result in erroneous interactions. For example, in a manipulator control task the human operator may select a incorrect co-ordinate points leading to a 'false negative interaction' as the manipulator would fail to reject the false interaction or there may be cases where the human operator select a correct co-ordinate points but the robot chooses a wrong co-ordinate points/ignores the human operator controls due to uncertainties in robot software/hardware leading to a 'false positive interaction' as the robot rejects a true interactions.

To incorporate the demands due the false alarms, in our earlier work we extended the neglect tolerance model by introducing the notions false alarm time (FAT) and false alarm demand (FAD) as illustrated in Fig. 1. FAT is defined as the time spent over false alarm identification and robot performance recovery to the pre-false alarm level.

The scenario depicted in Fig. 1 starts just after the operator starts to service the target robot. The robot performance increases with human operator servicing the robot over time and saturates at some point for both tele-operation and semi-autonomous autonomy modes. In Fig. 1, IT is the period of interaction between human operator and the robot, NT is the period of neglect where the human operator ignores the robot, FAT_{TO} is the time spent over false alarm identification and recovery for tele-operation mode and FAT_{SA} is the time spent over false alarm identification and recovery for semi-autonomous mode. Acceptable performance is the minimum performance level that can be tolerated by the operator for a given task. There will exist more than one IT within a single task. Similarly, there will also be more than one NT and FAT within a single task. The figure above only depicts one NT-IT cycle with a false alarm occurring within this cycle.

https://doi.org/10.1017/S0263574710000251 Published online by Cambridge University Press

False alarms, both false negatives as well as the false positives negatively affect the robot performance, but the FATs are larger for semi-autonomous mode as compared to tele-operation mode due to the delay in the false alarm identification process in the latter. In tele-operation mode, as the operator controls the robot continuously any occurrence of false alarm is identified and rectified in a shorter time period whereas in semi-autonomous mode the operator controls the robot by specifying waypoints for the latter to navigate and so any false alarm that occurs during the neglect period can only be identified and rectified during next period of service thereby resulting in larger FAT.

FAD is the additional demand placed on the robot operator due to false alarms, it is defined as

$$FAD = \frac{\sum FAT}{IT + \sum FAT}. \tag{1}$$

FAT in Eq. (1) can be expanded as

$$FAD = \frac{\sum FAT_P + \sum FAT_N}{IT + \sum FAT_P + \sum FAT_N}, \tag{2}$$

where FATp is the false alarm time contributed by a false positive and FATn is the false alarm time contributed by a false negative. Robot attention demand (RAD) is the robot's average performance over an interaction cycle[21] and extended neglect tolerance model redefines RAD as

$$RAD = \frac{IT + \sum FAT}{IT + NT + \sum FAT}. \tag{3}$$

Task complexity is a measure of difficulty level of the robot task and it remains as a key factor in deciding the robot performance level and number of occurrences of false alarms. In our experiments in this paper, the task complexity is only a function of static obstacle density given by

$$OD = \frac{TO}{TA}, \tag{4}$$

where OD is the static obstacle density, TO is the total number of obstacles in the robot workspace and TA is the total area of the robot workspace, the area used in this paper was 24 square meter. Figure 2 shows the robot workspace utilized for the experiments presented in this paper. The workspace was divided into a 1 m × 1 m grid where the obstacle was placed. Each obstacle was a static cylinder of diameter in the range of 30–50 cm. The obstacles were randomly placed in any of the 24 grids and routinely changed for every experiment. But, task complexity can be further extended to include active obstacle density and terrain factors. The dotted line indicates a potential path for the robot to navigate from start to finish points. During the experiments, the operator was free to choose any path.

We conducted experiments with our real and virtual humanoid soccer robots, Robo-Erectus Junior to validate the extended neglect tolerance model for two tasks with varying complexity levels across tele-operation and semi-autonomous modes of autonomy.

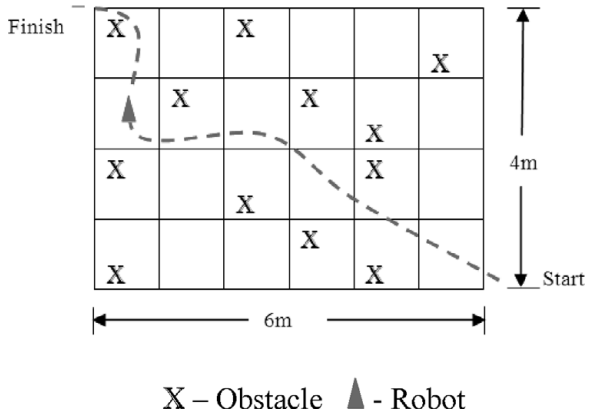


Fig. 2. Robot workspace.

3. Robo-Erectus Junior – A Soccer-Playing Humanoid Robot

This section introduces the Robo-Erectus Junior humanoid robot that we employed for our experiments for validating extended neglect tolerance model in this paper. Robo-Erectus Junior is one of the foremost leading soccer playing humanoid robots in the RoboCup humanoid leagues. The objective of the Robo-Erectus Junior development team is to develop a low cost humanoid platform for soccer robotics[22] and human robot interaction.[23] The mechanical structure, electronic control system and gait movement control of Robo-Erectus Junior has evolved through many stages to cope with the increasing complexity of the RoboCup humanoid leagues. Figure 3 shows the physical design of Robo-Erectus Junior.

Robo-Erectus Junior has been designed to cope with the complexity of a 3 versus 3 soccer game. Robo-Erectus Junior is equipped with three processors each for vision, artificial intelligence and control. Table I shows the specification of the processors used in Robo-Erectus Junior. The robot platform is equipped with three sensors: an USB camera to capture images, a tilt sensor to detect a fall, and a compass to detect their direction.[24] The servomotors used send back the feedback data including angular positions, speed, voltage, and temperature. To communicate with its teammates, Robo-Erectus Junior uses a wireless network connected to the artificial intelligence processor. The vision processor performs recognition and tracking of objects of interest including ball, goal, field lines, goal post teammate and the opponents based on a blob finder based algorithm.[25]

The further processing of detected blobs, wireless communications and decision making are performed by the artificial intelligence processor which selects and implements the soccer skills (like walk to the ball, pass ball, kick ball, and dive) the robot is to perform. Finally, the control processor handles the low level control of motor, based on the soccer skill selected by the artificial intelligence processor. Table II shows the physical specifications of Robo-Erectus Junior. It is powered by two high-current Lithium polymer rechargeable batteries, which are located in each foot. Each battery cell has a weight of only 110 g providing 12 v which means about 15 min of operation.

https://doi.org/10.1017/S0263574710000251 Published online by Cambridge University Press

Table I. Processor specification of Robo-Erectus Junior.

Features	Artificial intelligence processor	Vision processor	Control processor
Processor	Intel ARM XScale	Intel ARM XScale	ATMEL ATmega-128
Speed	400 MHz	400 MHz	16 MHz
Memory	16 MB	32 MB	4 KB
Storage	16 MB	16 MB	132 KB
Interface	RS232, WIFI	RS232, USB	RS232, RS485

Table II. Processor specification of Robo-Erectus Junior.

	Dimension			
Weight	Height	Width	Depth	Speed Walking
3.2 Kg	480 mm	270 mm	150 mm	5 m/min

We used both real and virtual humanoid robots so as to get more data for our experiments. Virtual robots were used as they are easier to set up, faster and more convenient for the human operators to use. Also, a virtual experimental set-up is far less expensive than real world set-up, therefore offering enormous opportunities for design exploration. Experiments with virtual robots also revealed the presence of false alarms both false positive and false negative interactions and therefore the associated false alarm demands in virtual environments for both autonomy modes. Our Virtual-RE simulator was used to perform experiments

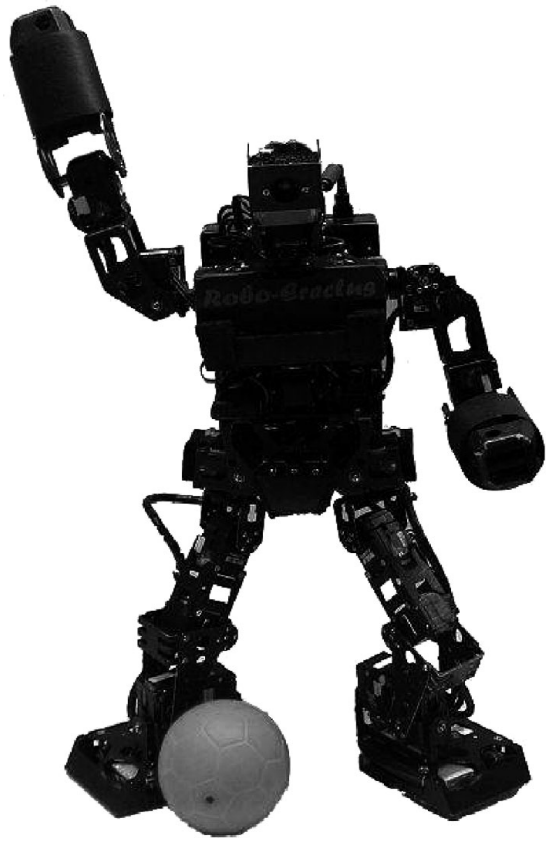


Fig. 3. Robo-Erectus Junior, the latest generation of the family Robo-Erectus.

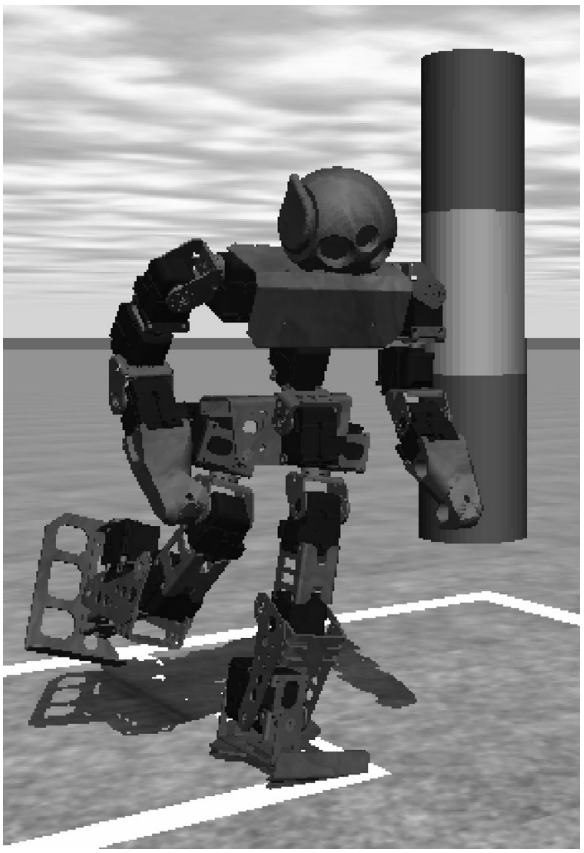


Fig. 4. Robo-Erectus Junior in virtual-RE simulator.

with virtual Robo-Erectus Junior humanoid robots providing several possibilities of visualization and interaction with the simulated world.[26] Figure 4 shows the virtual Robo-Erectus Junior humanoid robot and its environment. Virtual-RE simulator uses the Open Dynamics Engine (ODE) to simulate rigid body dynamics, which has a wide variety of features and has been used successfully in many other projects.[27] OpenGL libraries were used for both visualization and computation of imaging sensory information due to its effectiveness in accommodating modern hardware on a range of platforms.

Client-server based architecture was adopted for the realization of the simulator as it allows halting and stepwise execution of the whole simulation without any concurrencies. It also permits detailed debugging of the executed robot software. The simulation kernel models the robots and the environment, simulates sensor readings, and executes commands given by the controller or the user. The graphic user interface not only serves as a tool for interaction between

https://doi.org/10.1017/S0263574710000251 Published online by Cambridge University Press

the robot and the user but also visualize the robot status and feedback information whereas the all behavioural controls are handled by the robot controllers. In each simulation step, the controller reads the available sensors, plans the next action, and sets the actuators to the desired states. Virtual-RE provides each robot with a set of simulated sensors, i.e. tilt, compass, gyroscopes, camera images and motor feedback. The motor states are also simulated as in the real robot with feedback information that includes the joint angles as well as the velocities of motors.

4. Experiments

4.1. Experimental design

In these experiments, we validated the extended neglect tolerance model for two different levels of task complexities with our real and virtual Robo-Erectus humanoid robots across tele-operation and semi-autonomous modes of autonomy. We selected the task of navigating Robo-Erectus Junior in the soccer field towards a ball position. The robot and the ball were randomly placed in the soccer field. Operator used the graphic user interface to control the robots so as to navigate to the ball. Upon reaching the ball, the robot was placed at the initial position and the ball at another random position on the field for the next session. To validate the extended neglect tolerance mode for different task complexity levels, obstacles were placed in the soccer field where the robot navigated for the ball. The complexity was increased by increasing the obstacle density and therefore the task complexity. The secondary task for the operator was to control a second robot during the neglect time of the target robot so as to collect twice as much data per test session.

4.2. Instantaneous performance

In this paper, we redefined the instantaneous performance presented in ref. [28] to suit the task under study as ratio of current capability of the robot at a given time to the maximum capability of the robot. Instantaneous performance can take any value between 0 and 1. It is given by

$$P_I(t) = \frac{C_C(t)}{M_C(t)}, \tag{5}$$

where $C_c(t)$ is the current capability of the robot at time t for a task, $M_c(t)$ is the maximum capability of the robot or other objects at time t for the same task and $P_I(t)$ is the instantaneous performance at time t. In our experiments, the objective for the robot is to navigate to the ball position so the maximum capability would be the distance travelled by the robot moving optimally towards the ball position at top speed. We define maximum capability of the robot as

$$M_C(t) = K.\delta_t, \tag{6}$$

where δ_t is a small interval of time and K is the maximum speed of the robot. Since, Robo-Erectus Junior humanoid robots can travel at the speed of 8.33 cm/s, K value used was 8.33. The current capability of the robot is the actual distance travelled by the robot in the time δ_t:

$$C_C(t) = D_t - D_{t-\delta_t}, \tag{7}$$

where D_t is the distance travelled by the robot at time t and $D_{t-\delta_t}$ is the distance travelled by robot at time $t - \delta_t$. The instantaneous performance is computed as

$$P_I(t) = \frac{C_C(t)}{M_C(t)} = \frac{D_t - D_{t-\delta_t}}{K.\delta_t}. \tag{8}$$

4.3. Participants and procedure

The test subjects were first trained on the use of the graphic user interface to control the humanoid robots. Sufficient training was provided until the test subjects felt confident in using the user interface upon which the test session with real and virtual robots across tele-operation and semi-autonomous modes of autonomy for the two tasks were conducted. In the tele-operation mode, the operators controlled the robot continuously using a graphic user interface giving all commands and the robot possessed zero intelligence. In the case of semi-autonomous mode, the robot was capable of point to point navigation and simple obstacle avoidance based on sonar sensors and the human operator selected the way points for the robot to navigate and obstacle avoidance in cases where the robot failed. We recruited 20 test subjects aged between 18 and 51 and each of them took part in two 10 min session with real and virtual robots, so a total of 80 test sessions were performed. Of the 40 sessions each with real and virtual robots, 20 were dedicated to the tele-operation mode and remaining 20 to the semi-autonomous mode. Out of the 20 test sessions for both the autonomy modes, 10 sessions involved task 1 where the human operator navigated the robot to the ball with a robot workspace obstacle density of 0.5, and the other 10 sessions were dedicated to task 2, where the operator performed the same task but with a workspace obstacle density of 1. In each test session, the operator first serviced the target robot to accomplish the task of navigating to the ball. After servicing the target robot, he/she switches to the secondary task of navigating the second robot to the ball. In the semi-autonomous mode, the robot operator also intervened and provided additional controls every time the robot failed in task 2 where more obstacles where present. For example, if the robot failed the operator took control and provided additional controls to aid the robot in the obstacle avoidance process then the control was returned back to the robot for point to point navigation and obstacle avoidance. The operator performed the navigation task as many times as possible with the two robots during each 10 min test session. The instantaneous performance measurements together with the time, operator controls, and robot state information were recorded for each test session.

4.4. Results

Figure 5 shows the performance of the real and virtual robots for task 1 across tele-operation and semi-autonomous modes for all the 20 test subjects. False alarms were witnessed in 39 out of the total 40 test sessions with task 1 involving both real and virtual robots across tele-operation and

https://doi.org/10.1017/S0263574710000251 Published online by Cambridge University Press

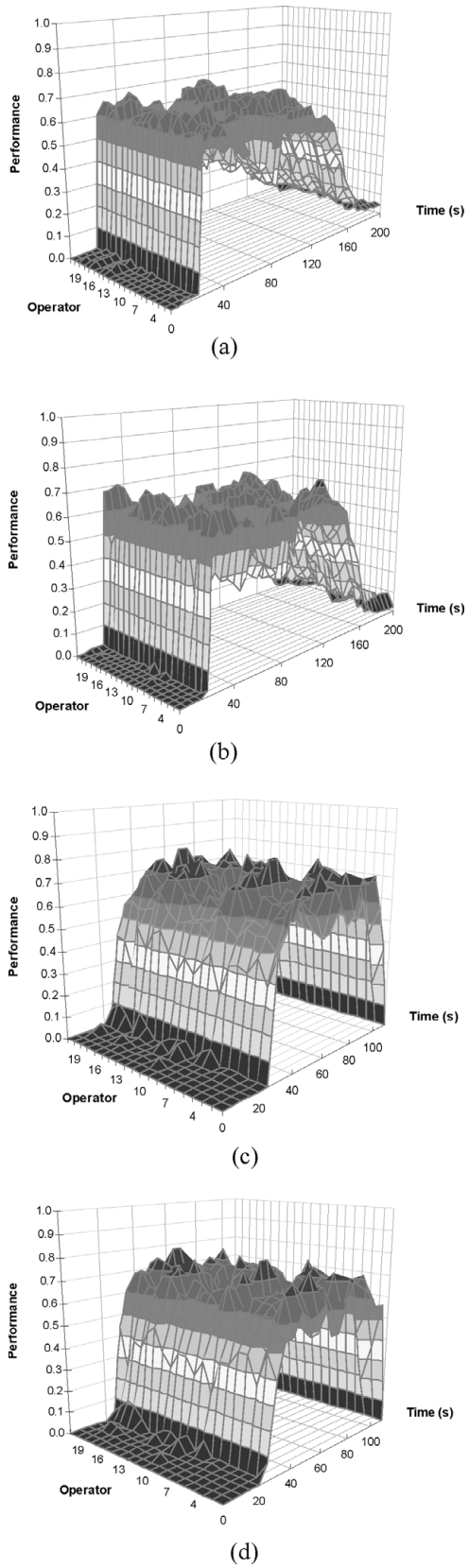


Fig. 5. Robot performance in human robot teams for task 1. (a) Real robot in semi-autonomous; (b) virtual robot in semi-autonomous; (c) real robot in tele-operation; and (d) virtual robot in tele-operation.

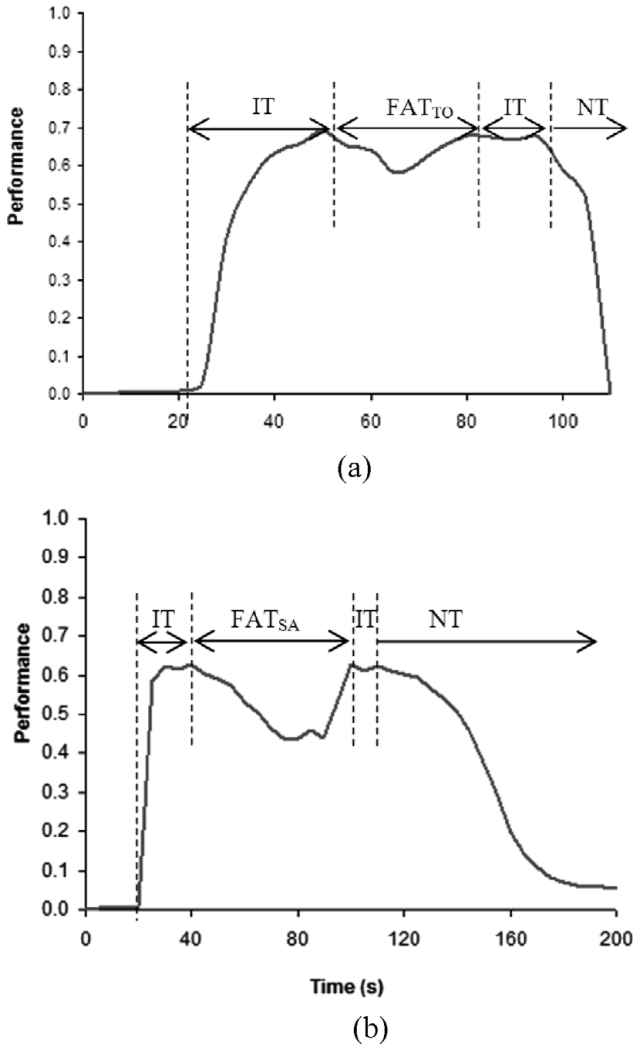


Fig. 6. Average robot performance in human robot teams for task 1: (a) real robot in semi-autonomous and (b) real robot in tele-operation.

semi-autonomous modes. A total of 68 false alarms were recorded out of which 22 were false negatives and 46 were false positives. In Fig. 5, as we move from left to right it is evident that the robot performance increases rapidly as the operator starts to operate the robot towards the ball and then stabilizes for both autonomy modes. Performance degrades with any occurrences of false alarms during robot operation. During the neglect period at the end of the IT-NT cycle, the performance drops abruptly to zero in the case of tele-operation mode as the robot possesses zero intelligence whereas in the case of semi-autonomous mode the performance drops gradually to zero.

As postulated, the FATs were found to be longer for the semi-autonomous mode as compared to tele-operation as any false alarms are identified and rectified early in the latter case. Figure 6 shows the average performance of the real robots for all twenty operators with event descriptors (IT, NT and FAT) for task 1 across tele-operation and semi-autonomous modes for clearer perception of the plots.

Figure 7 shows the performance of the real and virtual robots for task 2 across tele-operation and semi-autonomous modes for all the twenty test subjects. False alarms were

https://doi.org/10.1017/S0263574710000251 Published online by Cambridge University Press

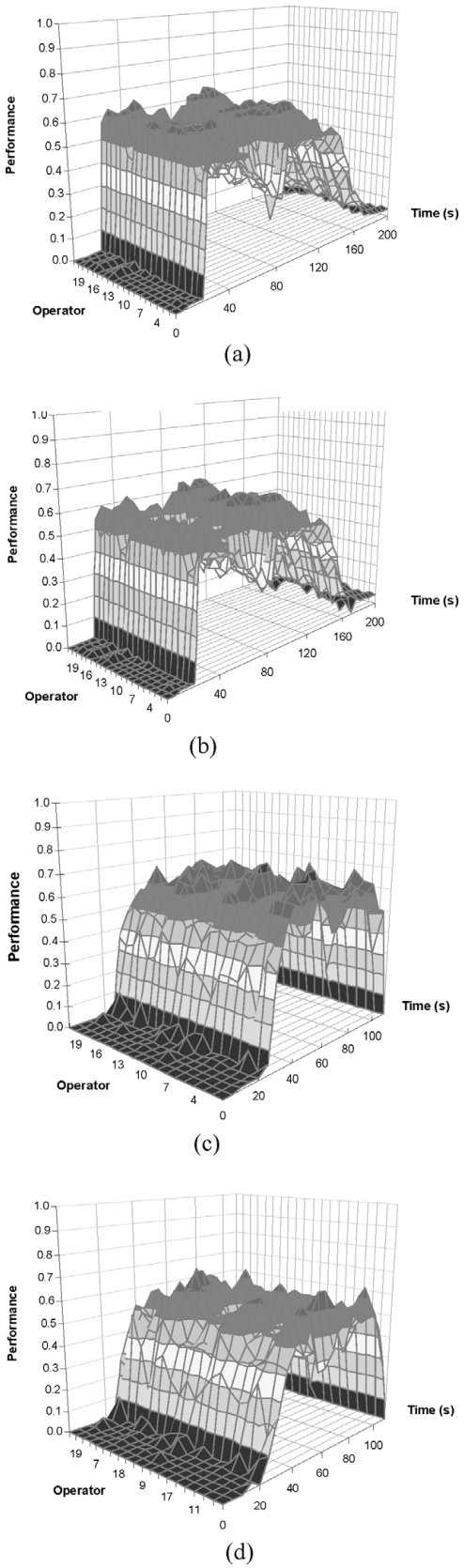


Fig. 7. Robot performance in human robot teams for task 2: (a) real robot in semi-autonomous; (b) virtual robot in semi-autonomous; (c) real robot in tele-operation mode; and (d) virtual robot in tele-operation mode.

witnessed in all the 40 test sessions with task 2. A total of 103 false alarms were recorded out of which 35 were false negatives and 68 were false positives.

In Figure 7, as we move from left to right the robot performance increases as the operator start operating the robot and then stabilizes. The performance drops abruptly to zero within 2 s of neglect period for tele-operation experiments whereas the performance drop during neglect period was more gradual for both the tasks across semi-autonomous experiments. During the neglect period, the rate of performance drop was slower in semi-autonomous mode as compared to tele-operation mode. Occurrence of false alarm degrades performance in all the experimental cases. The false positives witnessed in our experiments were mainly due to errors in the graphic user interaction scheme, software faults in robot's control and artificial intelligence modules and hardware failures in sensor/actuator systems.

The false negatives were mainly due to the human error pertaining to lack of understanding of the interaction scheme, and the task of interest. As postulated in the extended neglect tolerance model, the FADs for tele-operation were found to be shorter than those for semi-autonomous experiments for both task complexities. The performance results for real and virtual robots were found to follow similar pattern for both task complexities across both tele-operation and semi-autonomous modes. From the figures, it is evident that due to the increased complexity in task 2 attributed to the presence of additional obstacles in the path of the robot, the performance has significantly dropped in both real and virtual experiments.

For both the tasks complexities, tele-operation mode is efficient in increasing the performance of the robot upon servicing after a neglect period as compared to point to point mode. The performance drop due to false alarms are more prominent in semi-autonomous mode as compared to tele-operation mode as the period for performance recovery to pre-false alarm level is shorter in latter. With reduced neglect time in semi-autonomous mode, the performance recovery period can be lowered and therefore the performance drop can be reduced. But, any reduction in neglect time would be accompanied by increased RAD for the robot operator. For any given application, the performance drop-RAD trade-off has to be maximized. The trend of the graphs in Figs. 5 and 7 validate the extended neglect tolerance model for varying levels of task complexities. From the figures, it is evident that irrespective of the task complexity the tele-operation mode requires the operator to interact continuously with the robot as in the case of neglect the robot performance drops rapidly to zero.

Figure 8 shows the average human robot interactions required scheme for minimum acceptable performance level of 50% of peak value for task 1 for experiments with real and virtual robots across the two autonomy mode. The neglect time in semi-autonomous is far higher than that in tele-operation mode for maintaining a performance level of 50% of peak value. An increased neglect time allows operator to handle multiple robots or tasks thereby optimising resources and time while maintaining the performance above a certain threshold. Results of real and virtual robot experiments yielded similar results across tele-operation

https://doi.org/10.1017/S0263574710000251 Published online by Cambridge University Press

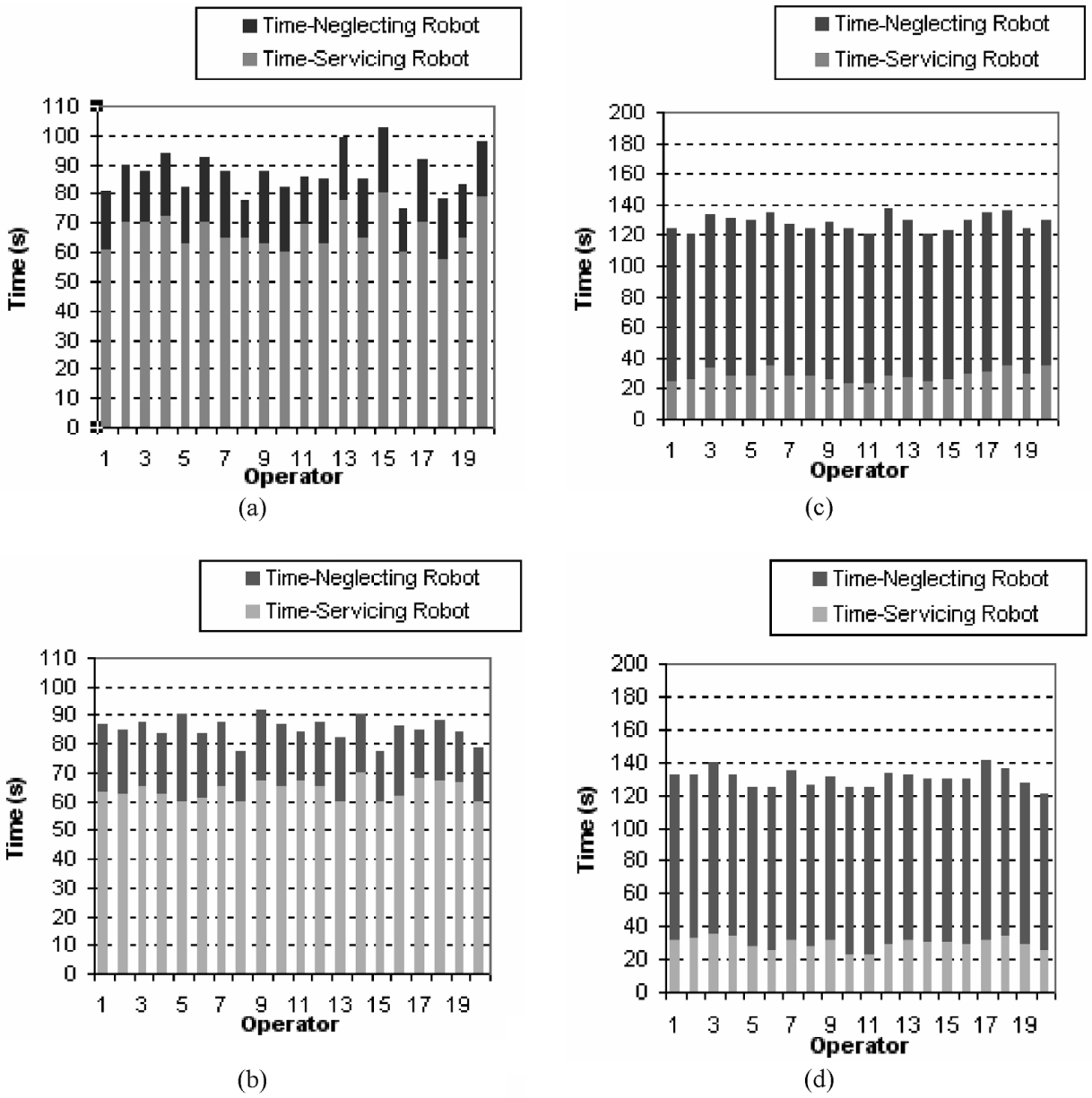


Fig. 8. Average interactions required by the interaction scheme for minimum acceptable performance level of 50% of peak value for real and virtual robots across the two autonomy modes. (a) Real robot in tele-operation mode; (b) virtual robot in tele-operation mode; (c) real robot in semi-autonomous mode; and (d) virtual robot in semi-autonomous mode.

and semi-autonomous modes. Figure 9 shows the average human robot interactions required for minimum acceptable performance level of 50% of peak value for task 2 with real and virtual robots across the two autonomy modes.

From Figs. 8 and 9, it is clear that the interaction time required for both tele-operation and semi-autonomous modes have risen with the task complexity level in task 2 as compared to task 1. This shows that for minimum acceptable performance at 50% level, task 2 requires more interaction time as compared to task 1 which directly implies more workload for the operator and lesser time for the secondary task. Figure 10 shows the RAD plotted against the average performance for task 1 across tele-operation and semi-autonomous modes. The figure presents the relationship between robot performance and operator workload in terms of RAD using the extended neglect tolerance model for task 1.

Tele-operation mode requires RAD closer to one as it requires the operator to continuously control the robot. No large variations were found in the data collected from the twenty operators both for real and virtual robot experiments. Figure 11 shows the RAD plotted against the average performance for task 2 for both autonomy modes. From the Figs. 10 and 11, it is evident that the tele-operation mode offers high robot performance as compared to semi-autonomous mode but tele-operation requires higher RAD as compared to semi-autonomous mode for both task complexities.

We also computed and compared the FADs for real and virtual robot experiments across the two autonomy modes for both the tasks. Figure 12 shows the average FADs for

https://doi.org/10.1017/S0263574710000251 Published online by Cambridge University Press

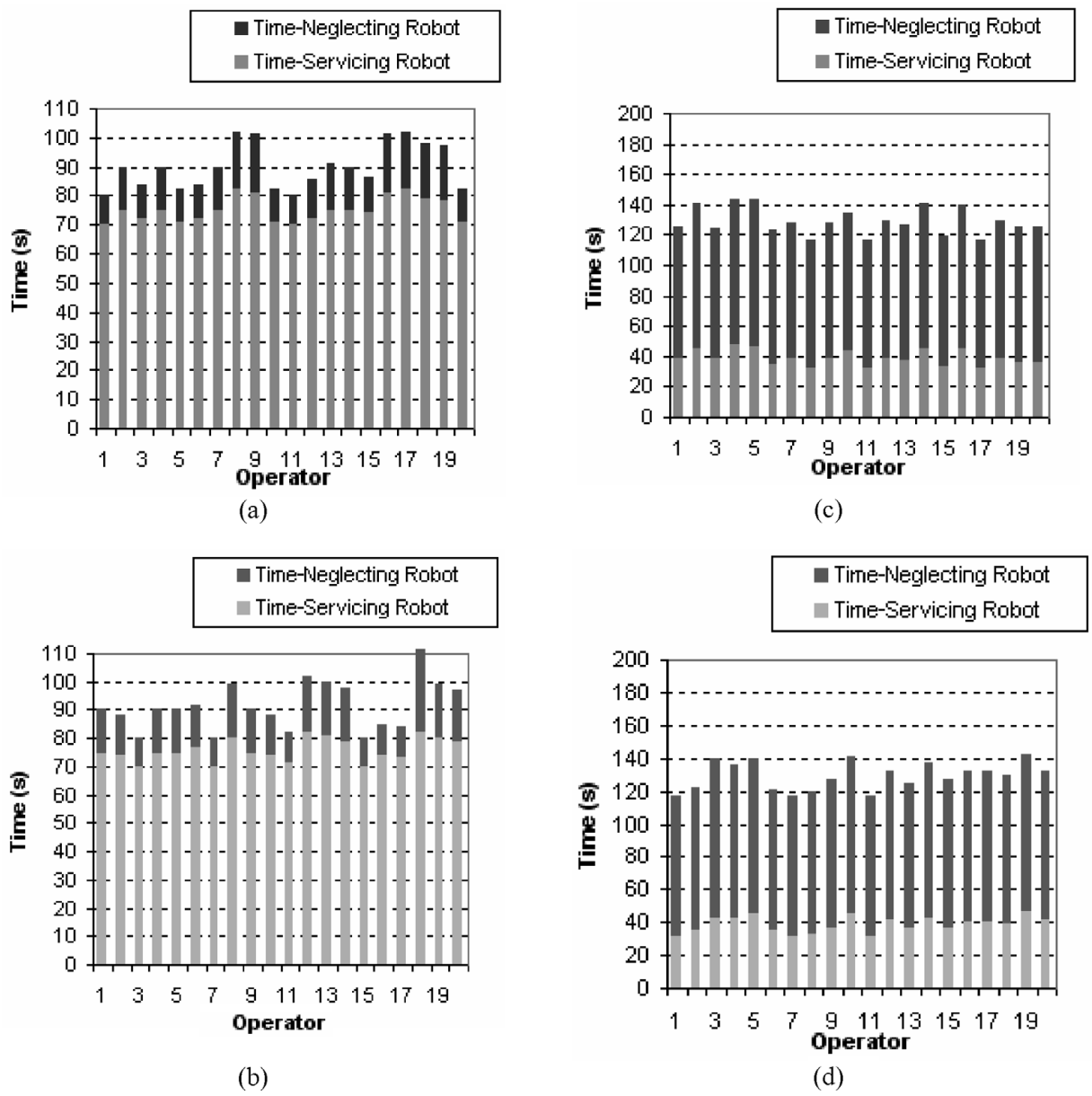


Fig. 9. Average interactions required by the interaction scheme for minimum acceptable performance level of 50% of peak value. (a) Real robot in tele-operation mode; (b) virtual robot in tele-operation mode; (c) real robot in semi-autonomous; and (d) virtual robot in semi-autonomous mode.

different experimental cases. The mean FAD for task 2 in semi-autonomous mode was highest for both real and virtual robot experiments.

It is clear from the figure that increasing task complexity increases the number of occurrence of false alarms and therefore resulting in higher FAD. The number of false alarms increased from 68 in task 1 to 103 in task 2, in specific the increase in false positives was more prominent and the results for real and virtual robot experiments followed the similar patterns. FADs can be used as a performance metric to gauge the additional operator efforts required for tasks of varying complexities and scenarios. Table III presents the percentage performance drop in task 2 in comparison to task 1 for all experimental cases. From, the table it is evident that an increase in task complexity results in performance drop and deriving this relationship for task of interest can aid robot operator optimise resources and time.

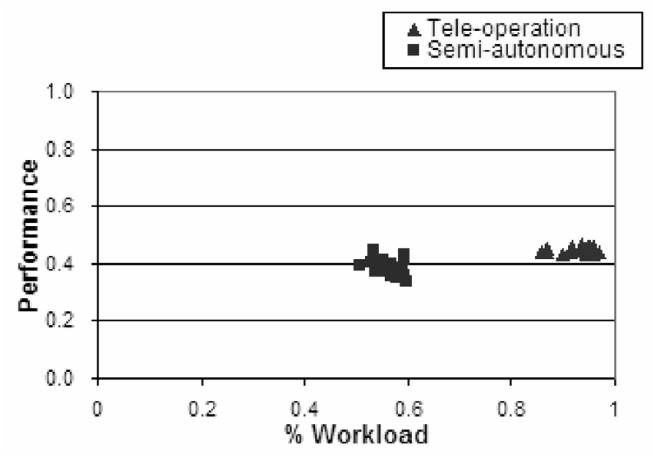
Table III. Percentage performance drop in task 2 in comparison to task 1 for all experimental cases.

Experimental cases	Performance drop
Real robot tele-operation	6.78%
Virtual robot tele-operation	10.75%
Real robot tele-operation	12.71%
Virtual robot rele-operation	11.27%

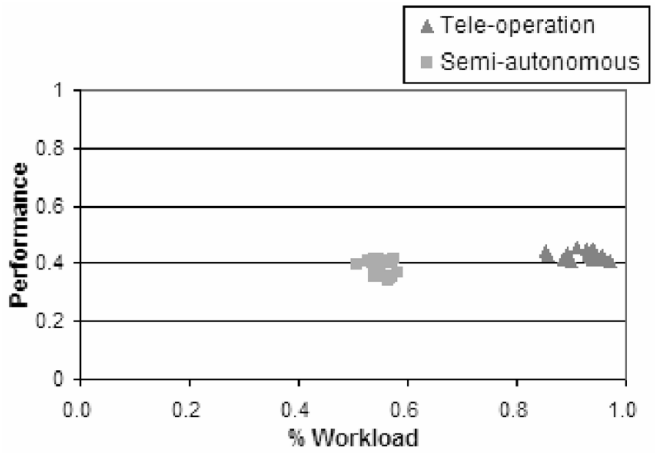
5. Conclusion

In this paper, we validated the extended neglect tolerance model for two robot navigation tasks with varying

https://doi.org/10.1017/S0263574710000251 Published online by Cambridge University Press

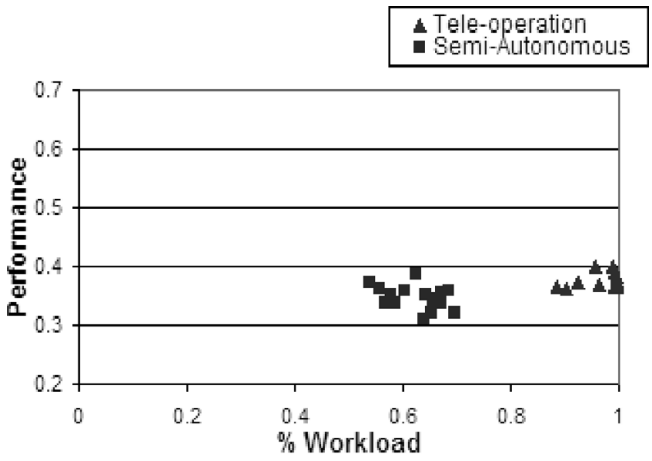


(a)

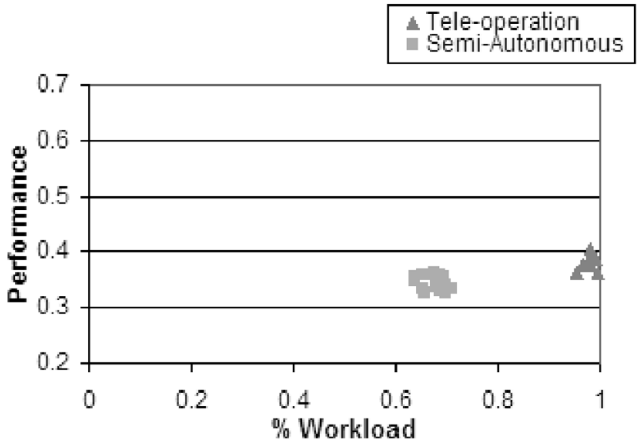


(b)

Fig. 10. RAD plotted against the average performance for Robo-Erectus humanoid robot using extended neglect tolerance model for task 1.



(a)



(b)

Fig. 11. RAD plotted against the average performance for Robo-Erectus humanoid robot using extended neglect tolerance model for task 2.

complexities across tele-operation and semi-autonomous modes of autonomy. Results of our experiments with real and virtual robots were largely consistent with the proposed extended neglect tolerance model predictions for both tasks across the two autonomy modes. FADs were found to be directly proportional to the task complexity, as the results showed that an increase in task complexity resulted in an increase in FAD. Irrespective of the task complexity, FADs were found to be higher in semi-autonomous mode as compared to tele-operation mode for experiments with real and virtual robots.

Results from both the tasks showed that tele-operation mode offers higher robot performance than semi-autonomous mode but the latter requires lower RAD and offers better performance deterioration rate during neglect times.

The experiments in this paper were limited to a human operator navigating a single robot towards a randomly placed ball.

Future work would include extending these results to estimating robot performance in multi-robot teams involving homogeneous and/or heterogeneous robots working together with a human operator towards accomplishing tasks of varying complexities. A second possibility of future work is to use FAD as a metric to compare performances of robot platforms, autonomy modes and interaction schemes for tasks of varying complexities. For the experiments detailed in the paper, the task complexity only accounts for the obstacle density and does not take into account the nature of the obstacle (static or dynamic) and terrain factors (even or uneven). For future work, we would be extending the task complexity to account for the obstacle nature and terrain factors and will be using dynamic obstacles and uneven terrain in our experiments.

Acknowledgments

The authors would like to thank staff and students at the Advanced Robotics and Intelligent Control Centre (ARICC) and higher management of Singapore Polytechnic for their support in the development of the Robo-Erectus Junior humanoid robots and its virtual simulator. In particular to

https://doi.org/10.1017/S0263574710000251 Published online by Cambridge University Press

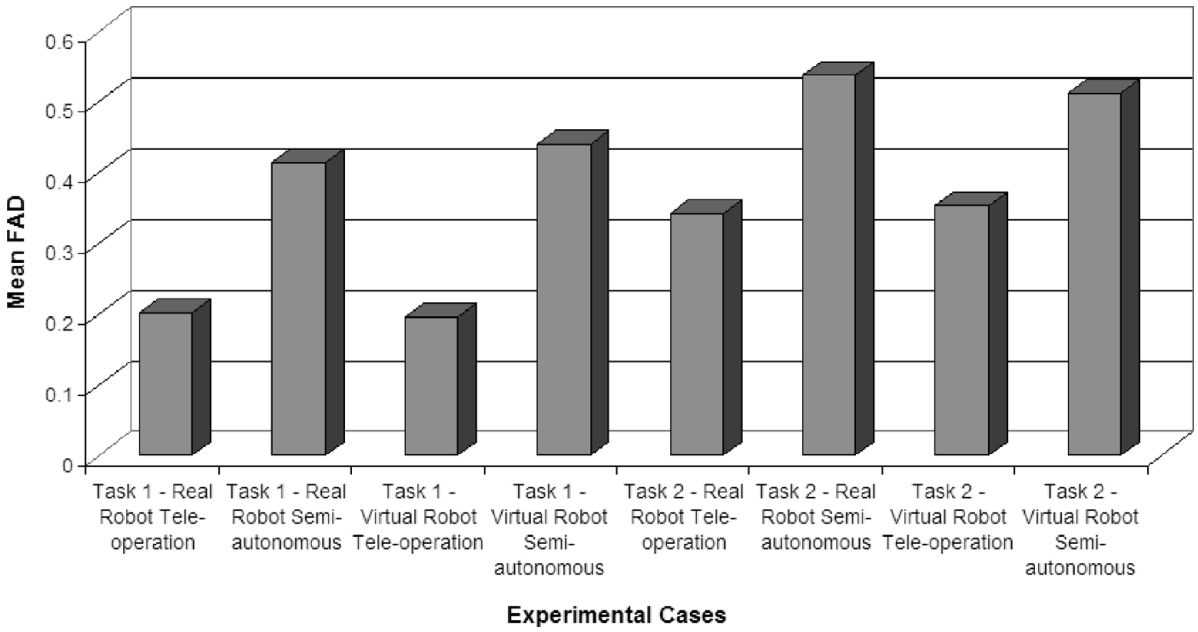


Fig. 12. Average FADs for different experimental cases.

Sunardi, Jiayin, Chen Ziyu, Fabian and Ngyun The Loan for their contributions to this project.

References

1. B. M. Hudock, B. E. Bishop and F. L. Crabbe, Development of a novel urban search and rescue robot, *United States Naval Academy Trident Scholar Report*, USA (2003).
2. G. S. Fischer, I. Iordachita, C. Csoma, J. Tokuda, S. P. DiMaio, C. M. Tempany, N. Hata and G. Fichtinger, "MRI-compatible pneumatic robot for transperineal prostate needle placement," *IEEE/ASME Trans. Mechatronics* **3**, 295–305 (2008).
3. K. Kyoungchul and J. Doyoung, "Design and control of an exoskeleton for the elderly and patients," *IEEE/ASME Trans. Mechatronics* **11**, 428–432 (2006).
4. M. Stein, Behavior-Based Control for Time-Delayed Tele-Operation *Ph. D dissertation* (Philadelphia, PA: University of Pennsylvania, 1994).
5. M. Alise, R. G. Roberts, D. W. Repperger, Jr CAM and S. Tosunoglu, "On extending the wave variable method to multiple-DOF teleoperation systems," *IEEE/ASME Trans. Mechatronics* **14**, 55–63 (2009).
6. K. W. Ong, G. Seet and S. K. Sim, "An Implementation of Seamless Human-Robot Interaction for Telerobotics," *J. Adv. Robot. Syst.* **5**(2), (2008).
7. M. Paul and A. Peter, "Shared Autonomy in a Robot Hand Teleoperation System," *Proceedings of International Conference on Intelligent Robotics Systems*, Munich, Germany (1994).
8. J. Wang, H. Wang, M. Lewis, P. Scerri, P. Velagapudi and K. Sycara, "Experiments in Coordination Demand for MultiRobot Systems," *Proceedings of IEEE International Conference on Distributed Human-Machine Systems*, Athens, Greece (2008).
9. J. W. Crandall, M. A. Goodrich, D. R. Olsen and C. W. Nielsen, "Validating human-robot interaction schemes in multi-tasking environments," *IEEE Trans. Syst. Man Cybern.* – Part-A **35**(4), 438–449 (July 2005).
10. J. W. Crandall and M. L. Cummings, "Identifying predictive metrics for supervisory control of multiple robots," *IEEE Trans. Robot.* **23**(5), (Oct. 2007).
11. J. W. Crandall and M. A. Goodrich, "Measuring the Intelligence of a Robot and its Interface", *Proceedings of NIST's Performance Metrics for Intelligent Systems Workshop*, Gaithersburg, MD (2003).
12. D. J. Bruemmer and M. Walton, "Collaborative Tools for Mixed Teams of Humans and Robots," *Proceedings of International Workshop on Multi-robot Systems*, Washington, DC (2003).
13. H. Hexmoor, "A Model of Absolute Autonomy and Power: Toward Group Effects," *Proceedings of AAAI Workshop Autonomy, Delegation, and Control: From Inter-Agent to Groups*, Alberta, Canada (2002).
14. J. Wang, Human Control of Cooperating Robots *Ph. D dissertation* (Philadelphia, PA: University of Pennsylvania, 2008).
15. R. E. Mohan, W. S. Wijesoma, C. A. A. Calderon and C. Zhou, "Experimenting false alarm demand for human robot interactions in humanoid soccer robots," *Int. J. Soc. Robot.* (Jan. 2009).
16. R. E. Mohan, W. S. Wijesoma, C. A. A. Calderon and C. Zhou, "Redefining Fan Out Metric: Estimating Human Capability in Controlling Multiple Robots," *IEEE/RSJ International Conference on Intelligent Robots and Systems*, St. Louis, MO (Oct. 2009).
17. R. E. Mohan, W. S. Wijesoma, C. A. A. Calderon and C. Zhou, "Validating Extended Neglect Tolerance Model for Human Robot Interaction in Search & Rescue Missions," *IEEE International Conference on Robotics and Automation*, Kobe, Japan (May 2009).
18. M. A. Goodrich, J. W. L. Crandal and J. L. Stimpson, "Neglect Tolerant Teaming: Issues and Dilemmas," *Proceedings of AAAI Spring Symposium on Human Interaction with Autonomous Systems in Complex Environments*, Stanford, CA (2003).
19. Steinfeld, T. Fong, D. Kaber, M. Lewis, J. Scholtz, A. Schultz and M. A. Goodrich, "Common Metrics for Human Robot Interaction," *Proceedings International Conference on Human Robot Interaction*, Salt Lake City, UT (2006).
20. D. R. Oslen and S. B. Wood, "Fan Out – Measuring Human Control of Multiple Robots," *Proceedings of SIGCHI Conference on Human Factors in Computing Systems*, Vienna, Austria (2004).
21. D. Olsen and M. Goodrich, "Metrics for Evaluating Human Robot Interactions," *Proceedings of NIST Performance Metrics for Intelligent Systems Workshop*, Gaithersburg, MD (2003).

https://doi.org/10.1017/S0263574710000251 Published online by Cambridge University Press

22. C. Zhou and P. K. Yue, *Robo-Erectus: A low Cost Autonomous Humanoid Soccer Robot* (Brill, Japan, 2004).
23. R. E. Mohan, C. A. A. Calderon, C. Zhou and P. K. Yue, "Extending NGMOSL model for human humanoid robot interaction in soccer robotics domain," *Appl. Bionics Biomech.* **5**(4), (2008).
24. C. A. A. Calderon, R. E. Mohan, C. Zhou, L. Hu and H. Hu, "Generating human-like soccer primitives from human data," *Robot. Autonom. Syst.* **57**(8), (2009).
25. C. A. A. Calderon, C. Zhou P. K. Yue, M. Wong and R. E. Mohan, "A distributed embedded control architecture for humanoid soccer robots," *Proceedings of 10th International Conference on Climbing and Walking Robots*, Singapore (2007).
26. C. A. A. Calderon, R. E. Mohan and C. Zhou, "Virtual-RE: A humanoid Robotic Soccer Simulator," *Proceedings of IEEE International Conference on Cyberworlds*, Hangzhou, China (2008).
27. R. Smith (Jan. 23, 2009). Open dynamics engine [Online]. Available: http://www.ode.org
28. J. W. Crandall and M. A. Goodrich, "Principles of Adjustable Interactions," *Proceedings of AAAI Fall Symposium on Human Robot Interactions*, Cambridge, MA (2002).

https://doi.org/10.1017/S0263574710000251 Published online by Cambridge University Press